Construction and Building Materials 77 (2015) 297–306

Contents lists available at ScienceDirect

Construction and Building Materials

journal homepage: www.elsevier.com/locate/conbuildmat

Characteristics of concrete/CFRP bonding system under natural tropical climate

Shukur Abu Hassan [a,*], Mehran Gholami [b], Yob Saed Ismail [a], Abdul Rahman Mohd Sam [b]

[a] Department of Applied Mechanics, Faculty of Mechanical Engineering, Universiti Teknologi Malaysia, Johor, Malaysia
[b] Department of Structure and Materials, Faculty of Civil Engineering, Universiti Teknologi Malaysia, Johor, Malaysia

HIGHLIGHTS

- The paper highlights strengthening concrete elements using CFRP plate.
- Concrete/CFRP bonding characteristics due to various environmental exposures have been evaluated.
- The influence of natural tropical climate on the bonding behavior was investigated.
- The effect of permanent stress on the bonding system has been assessed.

ARTICLE INFO

Article history:
Received 26 May 2014
Received in revised form 22 October 2014
Accepted 24 December 2014
Available online 12 January 2015

Keywords:
CFRP–concrete bonding
Bond characteristics
Bond durability
Tropical climate

ABSTRACT

Utilizing Carbon Fiber Reinforced Polymer (CFRP) composites for repairing, strengthening and upgrading concrete structures has been a very successful technique in recent years. Previous studies confirmed bonding CFRP plate to the concrete elements increased the mechanical performance such as flexural and shear resistance. However, the long-term bond integrity performance needs to be investigated further, focusing especially on the bond interfaces in various environmental conditions. In addition, little literature exists about the durability of the system in tropical climate. The current investigation is concerned with the behavior of concrete/CFRP bonding system in various environmental conditions focused on natural tropical climate which is an extremely hot/wet environment. Concrete/CFRP double lap joints prepared and subjected to diverse exposures. Pull-out tests conducted and the bonding characteristics investigated in detail. The results demonstrated the average bond strength of specimens subjected to tropical outdoor condition for 6 months deteriorated slightly.

1. Introduction

Deterioration caused by mechanical loading and weathering has forced many reinforced concrete structures all over the world need to be repaired and maintained throughout their service life. Besides, many of structures need upgrading to carry larger loads or must be strengthened according to new regulations codes. Using externally bonded metallic plates to strengthen and rehabilitate existing reinforced concrete structures have been a common method in construction industry for quite some time. The wide acceptance of FRP externally bonded system as a new technique for strengthening application is based on high quality, reliability and durability of such materials bonding system combined with rapid handling and assembly at site. Compared to steel plate system, the FRP composites is lighter and more durable to atmospheric and electro-chemical corrosion.

Using external CFRP strips to enhance the flexural behavior of reinforced concrete beams has been investigated thoroughly by many researchers [1–4]. In addition, shear and torsional strengthening of beams improved significantly through experimental and analytical studies [5–7]. Moreover, fatigue resistance of concrete elements strengthened with CFRP materials evaluated by experimental tests and numerical methods greatly [8,9].

However, the performance of bonding system in long term is still under investigation. Environmental factors such as temperature, moisture are the main factors influence the bonding during exposure. Previous durability studies has shown CFRP strengthening system were susceptible to the moisture [10–12]. Similarly, high temperature or thermal cycles influence the bonding system significantly [13–15]. Other factors have minor effects like as freeze/thaw [16], wet/dry cycles and chemicals (salt water and alkaline exposure) [12] and ultraviolet radiation (UV) [17].

* Corresponding author.
E-mail address: shukur@fkm.utm.my (S.A. Hassan).

http://dx.doi.org/10.1016/j.conbuildmat.2014.12.055
0950-0618/

Furthermore, durability of FRP material in Tropical climate environment investigated by some researchers [14,18,19].

The success of strengthening system depends highly on the CFRP–adhesive and concrete–adhesive interfaces. In fact, this issue influences the maximum flexural capacity and long-term performance of the strengthened member significantly [20–23].

According to literature [19,24], six failure modes of CFRP and concrete exist: failure of concrete, CFRP rupture, cohesive failure, delamination of CFRP, interfacial failure between CFRP and adhesive, and interfacial failure between adhesive and concrete. Obviously, debonding failure due to high interfacial stress causes considerable reduction in structural capacity [25]. Former experimental studies used single shear test [26] and double shear test or pull out test [27,28] to investigate about interfacial bonding behavior of FRP plated system. Likewise, it was shown the cracks develop due to high interfacial shear stress and normal stress at the plate cut-off point, at the end of the bonded plate and a distance away from the support [22].

The environmental resistance of any bonded assembly of FRP system depends on the durability of the individual components materials, as well as on the bond between them [21]. The changes in the adhesive and the adherend mechanical or chemical properties, respectively, modify the adhesion properties. Therefore, bond surface conditions and pre-treatments represent the key to enhancing the bond durability.

However, the long-term bond integrity performance needs to be investigated further, focusing especially on the bond interfaces in aggressive environmental conditions. In addition, the studies concerned about the durability of the system in Tropical climate are very limited. A numbers of experiments conducted to investigate short-term CFRP/concrete bonding performance around the world but very few studies focused on the combination of sustainable mechanical load and weathering conditions. Since the tropical climate experiences abundant rain and sunshine throughout the year, it would be essential to assess the long-term durability of the FRP plate-bonded system in this environmental condition. In this investigation, the bond characteristics of CFRP plate bonded to concrete prism exposed to tropical climate under sustainable pull–push load has been studied.

2. Experimental program

2.1. Material properties

The materials used in this study were concrete, CFRP and epoxy adhesive. A batch of concrete prism with the dimension of (100 × 100 × 300) mm was produced using the maximum coarse aggregate size of 10 mm with water/cement ratio of 0.47. The average compressive strength at 28 days was 47.37 MPa.

The pultruded CFRP plate, classified as type S (high strength), was supplied by Exchem EPC, United Kingdom. There were two pieces of CFRP plates bonded to both sides of a concrete prism. The plate dimensions were (555 × 50 × 1.4) mm. The mechanical properties are given in Table 1. The bonding system under the brand name of "Selfix Carbofibe" was a two-part epoxy adhesive consisted of a modified epoxy resin and inorganic fillers. The mixture was very viscous and light gray (almost white) in color. The epoxy system was difficult to mold due to its high viscosity and it took about 24 h to reach curing stage. The curing time was subjected to ambient laboratory condition. This epoxy adhesive consisted of two parts which were mixed with a ratio of 3:1. The typical mechanical and physical properties of epoxy adhesive are presented in Table 2 as stated in the supplier's specification.

Table 1
Typical mechanical properties of CFRP Plate.

	Tensile strength (MPa)	Tensile modulus (GPa)	Ultimate tensile strain (με)	Poisson's ratio (υ)	Fiber volume (%)
Manufacturer data	2800	150	Na	Na	70
Laboratory test (*)	2580	135	18,500	0.28	Na

Table 2
Typical mechanical and physical properties of epoxy adhesive.

Property	Value
Compressive strength (MPa) aged of 7 days at 20 °C	90
Tensile strength (MPa)	23
Thermal expansion/°C	33 e−6
Tensile modulus (GPa)	10
Shear modulus (GPa)	Na
Single lap shear strength (MPa)	>18
Glass transition temperature (DMTA) °C	>65
Water absorption	0.4%

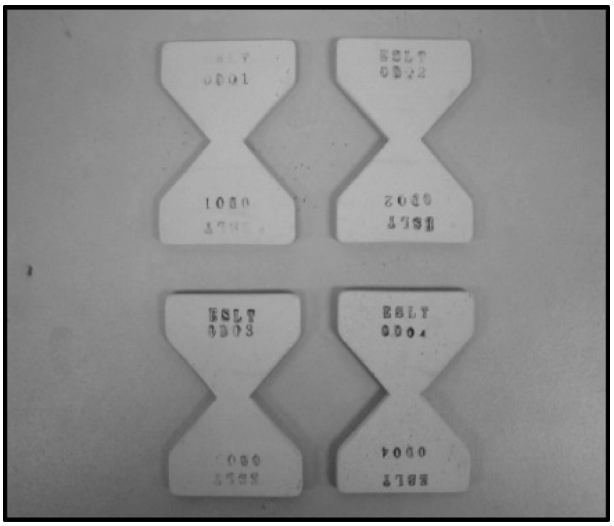

Fig. 1. Epoxy adhesive specimens.

2.2. Specimens detail

Three types of specimens considered in the experimental program: CFRP coupons, epoxy adhesive specimens, and double-lap concrete/CFRP joints. The CFRP coupons prepared based on ASTM D3039/3039M [29] with the dimension of (250 × 15 × 1.4) mm. Meanwhile, in order to overcome premature failure aluminum tabs were bonded to both sides of the specimen. In addition, the two parts epoxy adhesive was cast in a closed metal mold to produce butterfly shaped specimens based on Arcan shear method testing [30]. The mixing process was performed in the laboratory control room where the temperature and relative humidity were in the range of 24–26 °C and 40–55%, respectively. The specimens were left in the laboratory for 24 h for full chemical reaction prior to demolding. Then, all the specimens were conditioned in room ambient with a temperature ranging from 25 to 33 °C and relative humidity of 70–90% for 7–14 days to ensure the specimens were fully cured. The specimen size of 60 mm long and 45 mm wide with an average thickness of 4.4 mm was used for the experimentation study as shown in Fig. 1.

The concrete/CFRP specimen configuration demonstrated in Fig. 2 provides information regarding to specimen's geometry and location of strain gauges. The prepared specimen consisted of CFRP plates, concrete prism and epoxy adhesive to form a complete double-lap joint. Besides, a special rig was designed, fabricated and assembled in the laboratory to fulfil the experimental program (Fig. 3). Totally, a number of 15 CFRP coupons, 25 epoxy adhesive specimens and 27 concrete/CFRP double lap shear joints were prepared for the experimental program.

2.3. Environmental conditions

The environmental conditions and the number of specimens considered for the study are presented in Table 3. The specimens were prepared and subjected to environmental conditions including natural tropical climate, wet/dry cycles in plain water, wet/dry cycles in salt water, and laboratory condition up to 6 months. The outdoor exposure was "Natural Tropical in Malaysia". The temperature and relative humidity fluctuated between 23–35 °C and 60–95%, respectively during the time of study [31]. Fig. 4 shows the specimens exposed to natural environment. Besides, in the laboratory exposure condition, the specimens were experiencing 75–90% relative humidity and 25–32 °C of room temperature. Meanwhile, the wet/dry condition included 7 days wet followed by 7 days dry cycles.

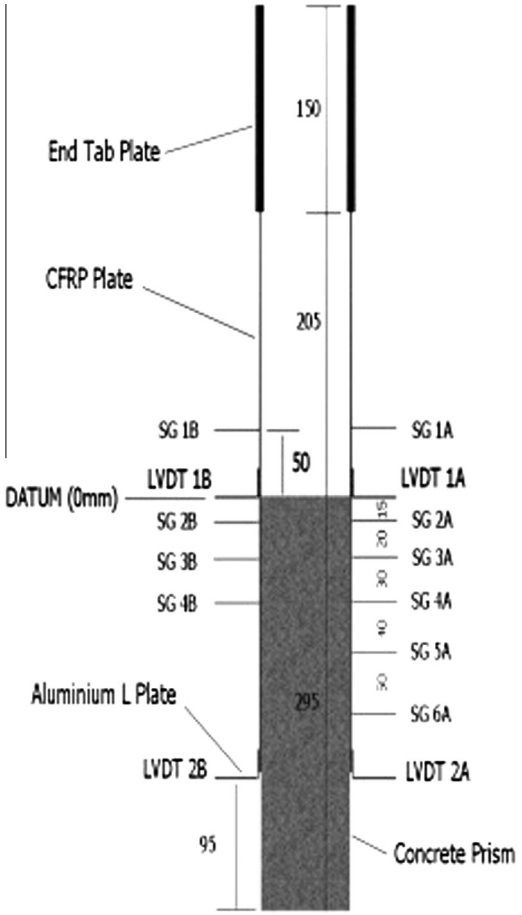

Fig. 2. Concrete/CFRP specimen and gauges.

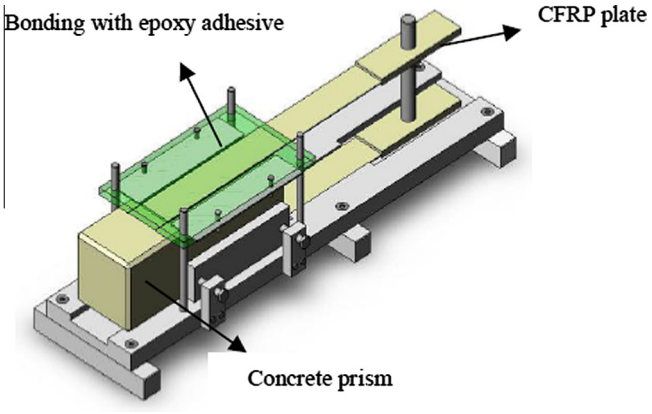

Fig. 3. Special rig to prepare concrete/CFRP specimens.

In addition, a number of concrete/CFRP specimens were subjected under loading around 40–50% of ultimate failure load during exposure. The main objective of the permanent stress on these specimens was to compare the effect of exposure condition on bonding strength for stressed and unstressed specimens. The test specimens were well equipped with standard strain gauges and a loading machine to detect comprehensive data during pre-stressed and experimental tests. Fig. 5 illustrates the specimen under sustained loading.

2.4. Bonding process

Proper surface preparation plays a main role to provide a durable bonding. It should be enough rough and clean from any dust and contamination. Therefore, the concrete prism surface was prepared through removing cement's rich layer using air tool hammer. The bonding process was carried out using a special rig which was designed to control the bonding alignment, bond pressure and adhesive thickness by maximum of 1 mm. The bonded CFRP plate was left in the fixture 24 h in room temperature and then maintained in room temperature at least two weeks for adhesive curing.

2.5. Pull out test set-up

The concrete/CFRP specimens were well equipped with standard strain gauges as demonstrated in Fig. 2. Moreover, four units of LVDT transducers brand TML with the sensitivity of 500 μ/mm and maximum displacement of 25 mm were installed at both parallel sides at the top (stressed end) and bottom (free end) of the test specimen. These instruments were used to measure a relative displacement and bond slip between CFRP plates and concrete prism during loading. The Instron Universal Testing Machine Series IX Model 4206 was used to create the loading shear mode within the materials system illustrated in Fig. 6. The tests were carried out in the loading speed rate control mode.

The static tensile load was applied monotonically until failure by a constant rate of 1 mm/min to represent quasi-static loading mode to the test specimen. The compressive static force applied onto the concrete prism surface was transferred by a set of roller bearing. The CFRP plate strain and bond slip data were recorded at every 5 kN load level up to failure. The recorded average strain from both sides of CFRP plates was analyzed to determine the specimen bond stress characteristic. The LVDT transducers were taken off around 40 kN to avoid the instruments being damaged at failure.

3. Experimental results and discussion

3.1. CFRP coupons test results

The tensile tests conducted for CFRP coupons with the speed rate of 2 mm/min. In general, the test results showed linear stress–strain behavior up to failure and failed in the same mode as control sample except for plain water and salted water groups which showed quite a significant effect of exposure condition. According to the results displayed in Figs. 7 and 8, all the exposed CFRP coupons showed a sign of degradation due to moisture absorption. The influence of moisture increased the value of Poisson's ratio for some exposed coupons, especially the ones exposed to salt water.

The results indicate the strength reduction around 10% for wet/dry specimens (CPLTUS-PW) from 2414 MPa to 2192 MPa. Furthermore, the stiffness of these coupons decreased from 135 GPa to 131 MPa which demonstrated almost 3% reduction. The strength and stiffness of outdoor coupons (CPLTUS-OD) reduced slightly 0.3% and 3%, respectively. It means the tropical climate did not influence the CFRP properties significantly. Moreover, the results represent the strength and modulus of salt water coupons (CPLTUS-SW) declined considerably around 9% and 15%, respectively. This issue indicated wet/dry in salt water degraded the mechanical properties severely compare to other environmental conditions. In fact, the strength reduction was due to the penetration of salt particles accompanied with moisture into the CFRP material. The crystallization of salt during wet/dry conditions might defect the resin matrix severely and caused debonding at the fiber–resin interfaces. Besides, the chemical attack of chloride ions intensified the strength degradation and weakened the shear capability in transferring stresses within the fiber-matrix system. In addition, water absorption made swelling and plasticization of the resin matrix which led to more ductile behavior and reduced the tensile stiffness gently [32].

Further, the coupons subjected to the laboratory ambient indicate a slight increase around 2% in strength. Nevertheless, the stiffness decreased approximately 3% due to humidity absorption. This means in a moderate temperature and humidity the CFRP properties are relatively constant. Overall, exposure to salt water condition was classified as the most aggressive, which the effect had contributed to the reduction in tensile strength, tensile modulus. Besides, outdoor exposure made slight changes in mechanical properties of CFRP coupons.

Table 3
Environmental conditions.

Sample type	Sample code	Number of specimens/Exposure conditions			
		Laboratory	Outdoor	Salt water (wet/dry)	Plain water (wet/dry)
CFRP plate	CPSTUS (Control)	3			
	CPLTUS (unstressed)	3	3	3 (24 cycles)	3 (24 cycles)
Epoxy adhesive	ESST (Control)	5			
	ESLT (Exposed)	5	5	5 (24 cycles)	5 (24 cycles)
Concrete/CFRP	BOSTUS (Control)	3			
	BOLTUS (unstressed)	3	3	3 (24 cycles)	3 (24 cycles)
	BOLTALS50 (stressed)	3	3	3 (24 cycles)	3 (24 cycles)

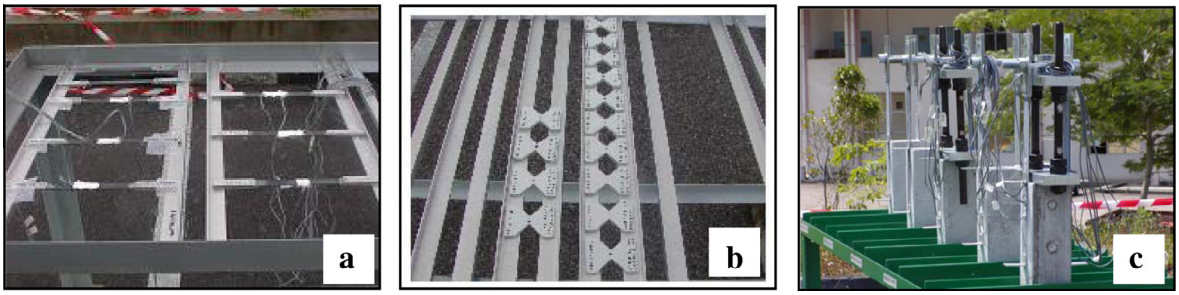

Fig. 4. The specimens exposed to outdoor condition (a) CFRP, (b) Epoxy adhesive, (c) CFRP/concrete.

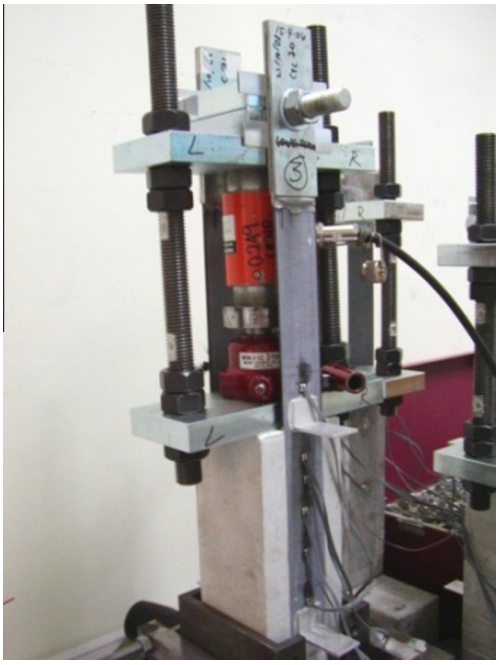

Fig. 5. Concrete/CFRP specimen under sustained loading.

Fig. 6. Pull out test set up.

3.2. Epoxy adhesive test results

Arcan method test conducted to find the shear strength and stiffness of the epoxy adhesive specimens. Figs. 9 and 10 show the specimen in Arkan grip and the test set-up. The loading rate was set-up to 1 mm/min and the specimen was loaded up to failure.

Table 4 presents the results in detail. Based on these results, the specimens' shear strength was reduced effecting from the exposure to wet/dry cycles in plain and salt water. The maximum moisture absorption recorded for salted water specimen which was around 2.67%. Meanwhile, the chemical chain of the epoxy weakened as the water penetrated through diffusion mechanism. Further, the outdoor specimens showed the highest shear strength around 23.85 MPa. The main factor influenced the shear strength was the oxidation process for outdoor specimens, as the weight reduced about 0.10% with yellowish effect. The epoxy shear strength versus exposure conditions is shown in Fig. 11.

Obviously, the shear strength for all the specimens was lower than control specimen. The plain water specimen had the lowest shear strength around 19.88 MPa, which was 32% lower than

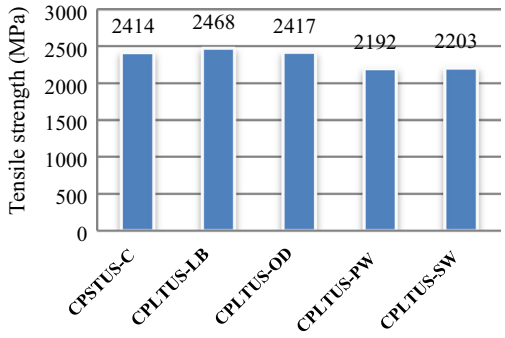

Fig. 7. Tensile strength of CFRP coupons after exposure.

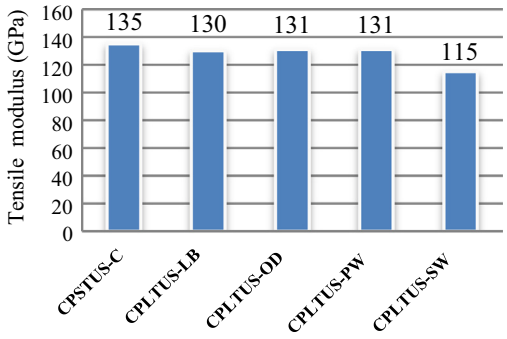

Fig. 8. Tensile modulus of CFRP coupons after exposure.

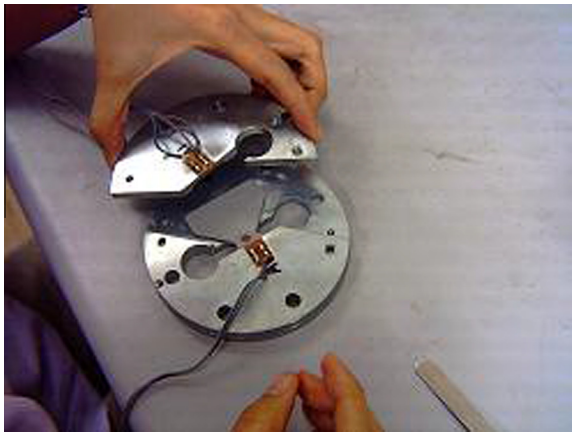

Fig. 9. Arcan male grip attached onto female grip.

control specimen, followed by salt water, Laboratory, and outdoor specimens which were 26.6%, 25.4%, and 18.4% lower than control specimen, respectively. Likewise, the shear modulus of epoxy adhesive coupons reduced around 9–14% after exposure to different conditions. Evidently, water absorption caused swelling and softening of the epoxy adhesive and decrease the stiffness gradually. Even in laboratory ambient the stiffness reduced significantly due to high relative humidity. The most degradation of stiffness was recorded for salt water coupons approximately 14% lower than control specimens. The epoxy shear modulus versus exposure conditions is shown in Fig. 12.

Basically, it was found using the Arcan test method was reliable, as the shear stress and strain relationship was linearly propagated. In addition, the formation of micro-porosity during casting process was difficult to be eliminated due to the geometrical effect of epoxy composition materials leading to air entrapment and finally

Fig. 10. Set-up of Arcan fixture to the loading machine.

reduced the epoxy cross-sectional area of the significant section. This effect accelerated the moisture diffusion process into the epoxy system. Moreover, all specimens failed in brittle form.

3.3. Concrete/CFRP specimens test results

The pull out tests conducted for three main sample group (BOSTUS, BOLTUS and BOLTALS50) to investigate concrete/CFRP bonding behavior. The test results focused on three subjects: (i) effective bond length, (ii) stress–slip relationship, and (iii) Stress distribution.

3.3.1. Effective bond length

Effective bond length is a part of bonding which transfer the stresses between concrete and plate entirely. In this study, the effective bond length was studied thoroughly for different specimens to find the influence of environmental conditions on the bonding characteristics. The transfer of load from CFRP plate to the concrete at low load level was fairly linear in control specimens (BOSTUS) and occurred at almost uniform rate. At this stage, the effective bond length was quite short. However, when the applied load increased up to failure, it was noticed the load transfer distribution became much more non-uniform and non-linear. For instance, at 10 kN load level, the effective length was about 105 mm, while at 20 kN load level it increased to 155 mm. Fig. 13 demonstrates local load versus bond length for BOSTUS-C03. The bond length characteristics were in agreement with previous studies conducted by Mukhopadhyaya [23], Bizindavyi [33] and Chajes et al [34].

This rapid change was probably due to the formation of micro-cracks or debonding at concrete–adhesive interface. This implied that no load had been transferred at the debonding region with further increment of applied load especially at bond stressed region of 0–35 mm. This can be referred to the curve of SG2, where it intersects with SG1 curve at about 45 kN of total applied load demonstrated in Fig. 14. It showed within the range of 45–50 kN of load level, both locations received the same amount of local strains value which signified the local debonding within the bond region.

Likewise, for BOLTUS group of specimens, the load transfer at low load level was fairly linear and occurred at a uniform rate demonstrated in Fig. 15. However, the effective length was increased up to full bond length as the load increased up to failure and the local load transfer distribution became much more non-uniform and non-linear. At failure load level the transferring of force from CFRP plate reached their maximum capacity when the full bond length was effectively transferred up to full debonding. Further, the progress of debonding was highly accelerated at failure load

Table 4
Detailed results of epoxy adhesive specimens shear tests.

Exposure condition	Shear strength (MPa)	Shear modulus (GPa)	Weight gain (%)	Weight loss (%)
Controlled	29.24	2.97	–	–
Laboratory	21.82 (−25%)	2.59 (−13%)	0.11	–
Outdoor	23.85 (−18%)	2.7 (−9%)	–	0.10
Plain water	19.88 (−32%)	2.64 (−11%)	0.25	–
Salt water	21.45 (−26%)	2.54 (−14%)	2.67	–

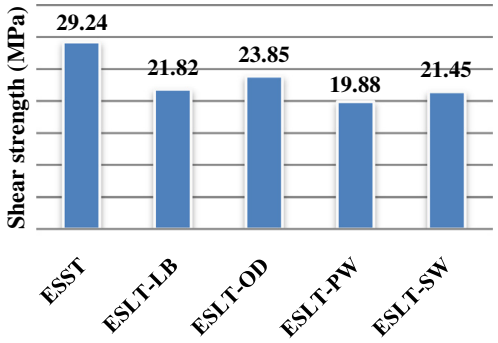

Fig. 11. Shear strength of epoxy adhesive versus exposure condition.

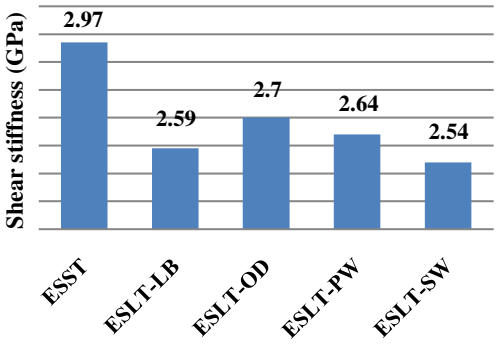

Fig. 12. Shear modulus of epoxy adhesive versus exposure conditions.

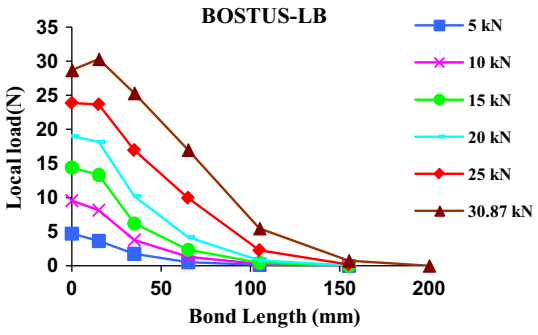

Fig. 13. Local load versus bond length for BOSTUS-LB.

for BOLTUS-OD, BOLTUS-PW and BOLTUS-SW. This could be referred to the bond force characteristics curve that became much more non-uniform and non-linear and indicated a strong influence of exposure condition on those specimens.

Likewise, the effective bond length for BOLTALS50 specimens was almost uniform at all load levels and did not show any sign of progressive debonding near to failure load. The effective bond length was highly constrained within 155 mm of whole bond

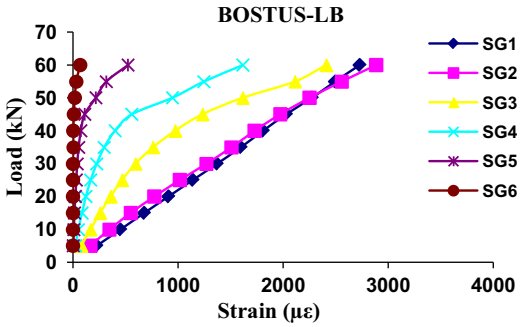

Fig. 14. CFRP plate load versus local plate strain for BOSTUS-LB.

length at failure load. This probably showed no sign of exposure effect or influences on the permanently stressed specimen during experiment. Overall, exposure to natural tropical climate affected the bonding length moderately, particularly before failure load.

3.3.2. Bond stress–slip relationship

Relative displacement at loaded end for BOSTUS-C03 shown in Fig. 16 provides a very consistent curve pattern of bond stress–slip relationship. It shows a perfect linear relationship between bond stress and bond slip at specimen loaded end up to 40 kN. The linear increment of bond slip indicates the shear deformation has occurred due to high stresses being built up around the bond region. The high relative displacement developed at loaded ends significantly was caused by the bond failure occurred in adhesive–concrete interfaces. In addition, all BOSTUS specimens showed almost equal deformation for 10 kN and 20 kN load level at specimen loaded ends and almost zero deformation at free ends. Meanwhile, the bond stress against bond slip characteristics above 20 kN plate load level was not recorded due to technical limitation.

Typical plots of average bond stress versus bond slip for BOLTUS specimens are shown in Fig. 17. Obviously, wet/dry cycles have significantly affected the bond performance for BOLTUS-PW group due to a higher relative deformation specimens both ends. The critical factor affected the non-linearity relationship of bond slip was concrete's uneven surface texture that formed mechanical interlocking at adhesive–concrete interface. This type of mechanical interlocking also increased the bond load due to resistance to both shear and tensile stresses [35].

Likewise, test results for BOLTALS50 specimens showed the debonding and local bond slip between CFRP plate and concrete has occurred at the most stressed and free ends for all specimens. From the results, it implied the load sustained and exposure conditions caused a significant shear deformation along bond interfaces of CFRP plate–epoxy and epoxy–concrete. Due to pre-stressing the bond slips produced at both sides were not really in agreement with each other. Besides, the wet–dry cycles applied to BOLTALS50-PW have significantly affected the bond performances. This effect was also experienced by BOLTALS50-SW. Meanwhile,

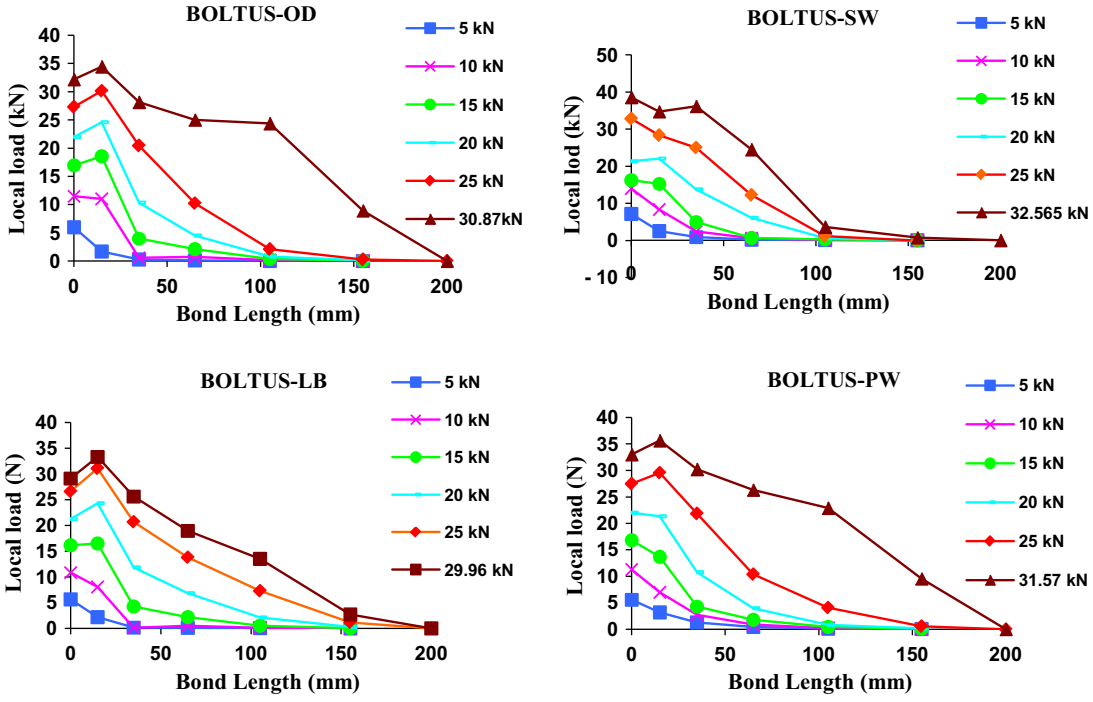

Fig. 15. Local load versus bond length for BOLTUS specimens.

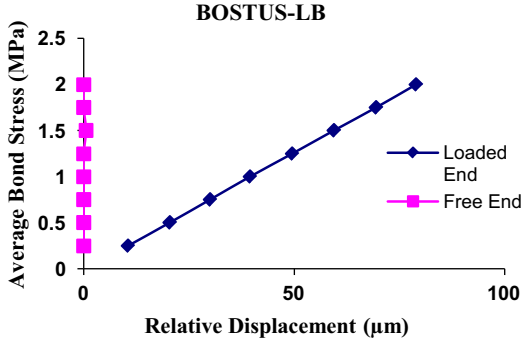

Fig. 16. Average bond stress versus relative displacement for BOSTUS.

BOLTALS50-LB and BOLTALS50-OD showed almost the same relative deformation at their stressed ends at 20 kN plate load level.

Overall, the non-linear behavior of bond slip for all exposed specimens was due to the uneven concrete surface profiles along the bond interfaces.

3.3.3. Stress distribution characteristics

Table 5 presents bond characteristics related to all concrete/CFRP specimens. The unexpected result is increasing the average of failure loads after exposure, especially for the specimens subjected to plain water and salt water approximately 7–15%. This issue can be explained by curing the concrete during exposure which caused increasing the shear strength of concrete surface. However, the average bond strength reduced slightly after exposure. Obviously, the reason was degradation of bonding during environmental exposure.

Local bond stress versus bond length for BOSTUS specimen demonstrated in Fig. 18. It shows the maximum local bond stress was 4.38 MPa, 7.95 MPa and 5.75 MPa at 10 kN, 20 kN and near to failure load, respectively. Refer to Fig. 19, the maximum local bond stress region shifted to a new adjacent location at a relative load level (F/Fmax) of about 0.3. Further, the bond stressed end region has initiated cracking at about 0.7 of relative load level (F/Fmax) with sudden increased in local bond stresses. The results were in agreement with Mukhopadhyaya [23] and Bizindavyi [33] investigations.

Moreover, for BOLTUL specimens the local bond stress distributions were higher near to stressed ends region (15–35 mm) at almost all load levels as illustrated in Fig. 20. At 20 kN load level, all the exposed specimens showed almost uniform local bond stress distributions along the bonded length. The maximum local bond stress occurred at near stressed end and reduced toward the free ends. The local peak bond stress occurred at 15–35 mm of bond length, reducing toward free end. At this load level, the bond integrity between CFRP plate–epoxy and epoxy–concrete interfaces was fully developed. Fig. 20 shows that the highest local peak bond stress was 12.19 MPa related to BOLTUS-OD, followed BOLTUS-LB, BOLTUS-PW and BOLTUS-SW. The BOLTUS-SW specimen presented the lowest value of local peak shear stress occurred at 20 kN and it clearly showed the toughness of CFRP plate was affected due to resin matrix failure.

The local bond stress distributions for all BOLTALS50 specimens showed almost the same characteristic of short bond transfer length at the 10 kN load level. Again, the maximum stress occurred at near the stressed end and decreased toward the free ends. Meanwhile, at the 20 kN load level, all the specimens showed almost uniform local bond stress distributions along the bond length. This indicated that a formation of bond integrity (or state of equilibrium) of CFRP plate–epoxy and epoxy–concrete interfaces had been reached. Finally, at the failure load level, the local bond stress distribution became much more non-uniform and non-linear for all the specimens. The local peak shear stress occurred at the 15–35 mm bond region and shifted to the adjacent region once the formation of interfaces bond failure had occurred. The BOLTALS50-PW and BOLTALS50-SW showed an almost uniform distribution of local bond stress at the final load level that was formed in the bond region of 15–105 mm.

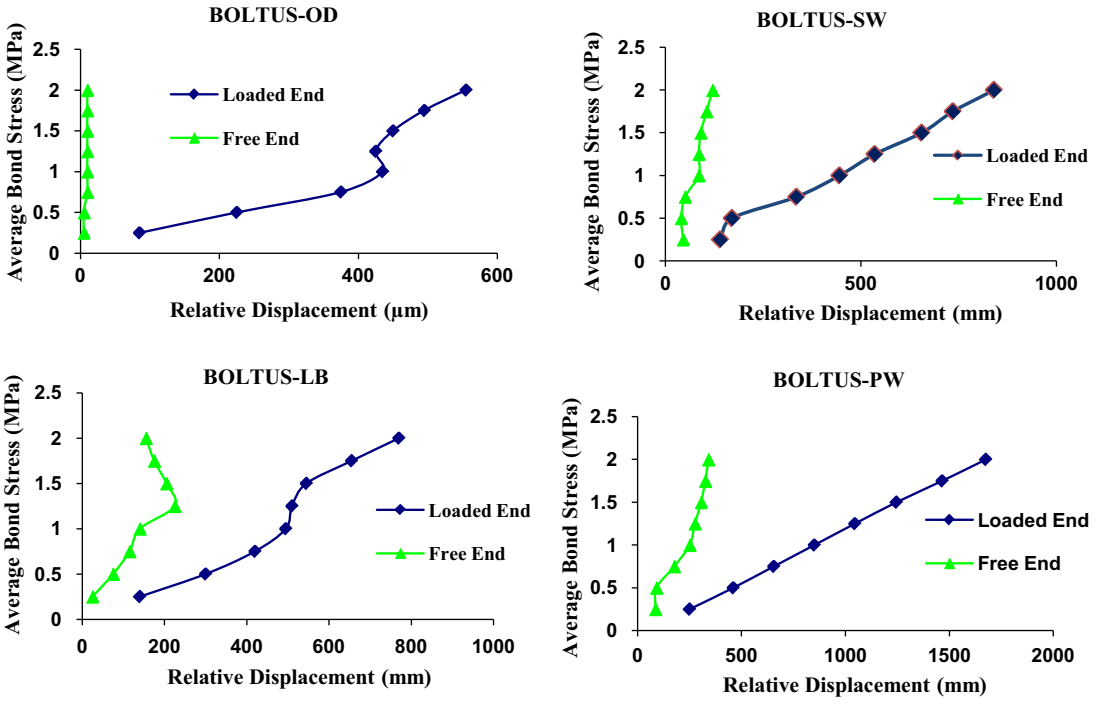

Fig. 17. Average bond stress versus relative displacement for BOLTUS specimens.

Table 5
Bond characteristics of the concrete/CFRP specimens.

Specimen	Exposure condition	Failure load (kN)	Peak load bond stress (MPa)	Average bond strength (MPa)
BOSTUS	–	60.15	12.34	3.01
BOLTAS	LB	60.09	6.78	3.01
	OD	58.86	7.51	2.94
	PW	64.27	5.70	3.21
	SW	64.13	5.88	3.21
BOLTALS50	LB	56.24	9.78	2.75
	OD	63.0	10.34	3.0
	PW	69.22	10.2	3.06
	SW	66.25	8.9	2.98

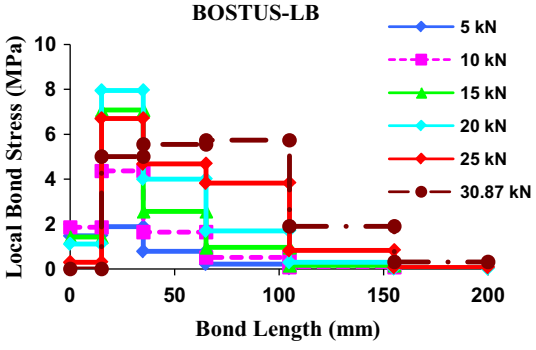

Fig. 18. Local bond stress versus bond length for BOSTUS specimen.

3.3.4. Failure mode

High strain energy was released during failure for BOSTUS specimen, followed by a very loud sound generated by the specimen. The full brittle failure was initially started by formation of cracking occurred at adhesive–concrete interface of the specimen. The full specimen debonding started after the formation of macro-cracking

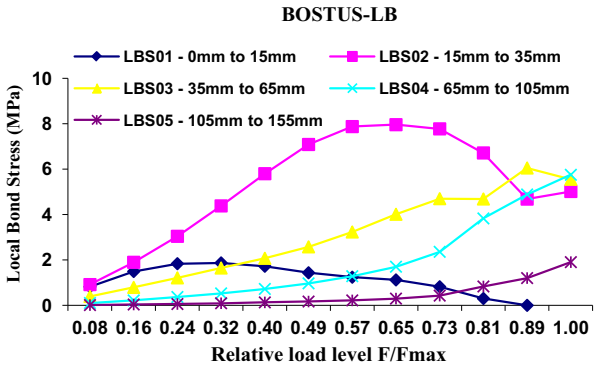

Fig. 19. Local bond stress versus relative load level for BOSTUS specimen.

at bond interface. The full bond failure occurred in a very short period indicated the sign of brittleness of the bond materials. The debonding failure was dominated by concrete shearing failure showed the weakness of concrete in shear or tensile properties compared to epoxy adhesive and CFRP plate. From observation made on the failure specimen (Fig. 21), no epoxy adhesive remained on the concrete surface and it showed the epoxy adhesive was much stronger than concrete under shear deformation.

Visual inspection of BOLTUS specimens indicated surface shearing cracks failure near the stressed end and toward the free ends. For BOLTUS-LB, BOLTUS-OD and BOLTUS-PW, the overall bond failures were equally formed by concrete shearing failure, and for BOLTUS-SW it showed a combination of concrete shearing failure and CFRP plate shear out failure from the bond region of 35 to 65 mm toward the free ends. The sign of brittle bond failure could be seen through the development of a high local bond stress level that had been produced in a very short period.

Likewise, visual inspection of all the respective failure of BOLTALS50 specimens indicated that a thick layer of concrete remained adhered on the CFRP plate due to concrete shearing

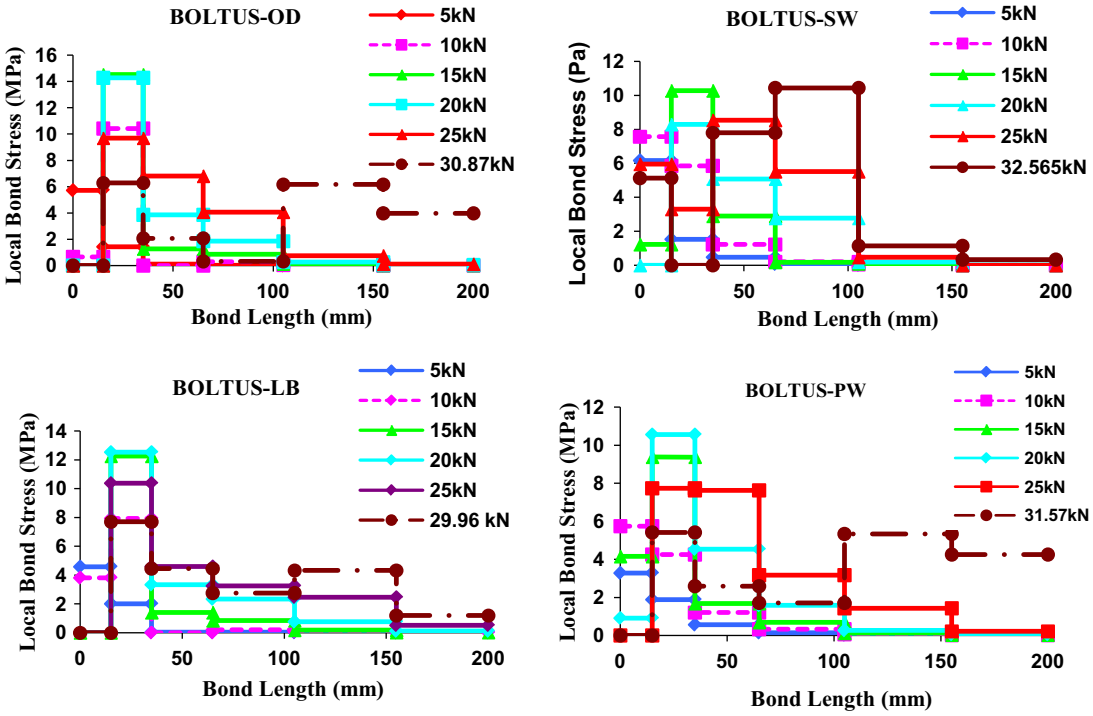

Fig. 20. Typical local bond stress distribution for BOLTUS specimens.

Fig. 21. Failure mode dominated by concrete shear failure.

failure. This formation has occurred on most of the stressed bond region of 0–65 mm. Furthermore, the outdoor condition influenced the specimen and caused yellowish effect on BOLTALS50-OD CFRP plate. Meanwhile, outdoor exposure condition caused the materials to become more brittle through oxidation process. The formation of rust on the BOLTALS50-SW surface was due to chemical reaction between saltwater and steel rig tie rods.

4. Conclusions

In this study, the behavior of concrete/CFRP bonding system was investigated and the bond characteristics after exposure in different environmental conditions were discussed in detail. Double lap joints of concrete/CFRP were prepared and subjected to various environmental conditions up to 6 months. Then, the specimens were loaded to failure under pull-out tests. The main objective was to investigate the effect of natural Tropical climate on the bond characteristics. Adhesive bonded joints were generally attacked by exposure to moisture and elevated temperature. A small amount of moisture induced plasticization of the adhesive in highly stressed regions and was beneficial in reducing stress concentrations. However, the mechanical properties of joints reduced due to the effects of environmental conditions on the adhesive itself. The major conclusions are as follow:

- Using the Arcan test method was reliable to find the epoxy adhesive properties. The most degradation was observed for wet/dry conditions in plain water and salt water. Besides, the strength and stiffness of epoxy adhesive specimens reduced 18% and 9% after 6 months exposure to natural tropical climate.
- The concrete was the critical part and the performance of the system related to its behavior. Although the CFRP plate and epoxy adhesive were affected by exposures, these materials demonstrated appropriate properties to transfer the stresses. The specimen's bond failure was dominated by concrete shearing failure showed the weakness of concrete in shear or tensile properties compared to epoxy adhesive and CFRP plate.
- The concrete/CFRP bonding system transferred stress in a linear uniform rate from CFRP plate to concrete at low load level for all specimen groups. While, at higher load level and near to failure, it became non-uniform and non-linear with local debonding initiating at the specimen's loaded end.
- The effective bond length was relatively short at low and medium load levels and progressively increased at failure load. Besides, the progress of debonding was highly accelerated at failure load level for all specimens group.
- The average of failure loads increased after 6 months exposure. While, the average bond strength reduced slightly due to degradation of bonding during environmental exposure. Actually, increasing the shear strength of concrete during exposure enhanced the failure load.

- Exposure to natural tropical climate affected the bonding system slightly. The average bond strength indicated little degradation and the stress distribution along the bonding showed a very close behavior to control specimens.

References

[1] Nguyen D, Chan T, Cheong H. Brittle failure and bond development length of CFRP–concrete beams. J Compos Constr 2001;5(1):12–7.
[2] Alagusundaramoorthy P, Harik I, Choo C. Flexural behavior of R/C beams strengthened with carbon fiber reinforced polymer sheets or fabric. J Compos Constr 2003;7(4):292–301.
[3] Li L, Guo Y, Liu F, Bungey J. An experimental and numerical study of the effect of thickness and length of CFRP on performance of repaired reinforced concrete beams. Constr Build Mater 2006;20(10):901–9.
[4] Dong J, Wang Q, Guan Z. Structural behaviour of RC beams with external flexural and flexural–shear strengthening by FRP sheets. Compos B 2013;44:604–12.
[5] Brena S, Macri B. Effect of carbon-fiber-reinforced polymer laminate configuration on the behavior of strengthened reinforced concrete beams. J Compos Constr 2004;8(3):229–40.
[6] Obaidat Y, Heyden S, Dahlblom O, Abu-Farsakh G, Abdel-Javad Y. Retrofitting of reinforced concrete beams using composite laminates. Constr Build Mater 2011;25:591–7.
[7] El-Ghandour A. Experimental and analytical investigation of CFRP flexural and shear strengthening efficiencies of RC beams. Constr Build Mater 2011;25:1419–29.
[8] Al-Rousan R, Issa M. Fatigue performance of reinforced concrete beams strengthened with CFRP sheets. Constr Build Mater 2011;25:3520–9.
[9] Xie J, Huang P, Guo Y. Fatigue behavior of reinforced concrete beams strengthened with prestressed fiber reinforced polymer. Constr Build Mater 2012;27:149–57.
[10] Chu W, Wu L, Karbhari V. Durability evaluation of moderate temperature cured E-glass/vinylester systems. Compos Struct 2004;66(1–4):367–76.
[11] Frigione M, Aiello M, Naddeo C. Water effects on the bond strength of concrete/concrete adhesive joints. Constr Build Mater 2006;20:957–70.
[12] Cromwell J, Harries K, Shahrooz B. Environmental durability of externally bonded FRP materials intended for repair of concrete structures. Constr Build Mater 2011;25:2528–39.
[13] Li G, Pang S, Helms J, Mukai D. Stiffness degradation of FRP strengthened RC beams subjected to hygrothermal and aging attacks. J Compos Mater 2002;36(7):795–812.
[14] Almusallam T, Al-Salloum Y. Durability of GFRP rebars in concrete beams under sustained loads at severe environments. J Compos Mater 2006;40(7):623–37.
[15] Galati N, Nanni A, Dharani L, Focacci F, Aiello M. Thermal effects on bond between FRP rebars and concrete. Compos A Appl Sci Manuf 2006;37(8):1223–30.
[16] Chajes M, Thomson J, Farschman C. Durability of concrete beams externally reinforced with composite fabrics. Constr Build Mater 1995;9(3):141–8.
[17] Kumar B, Singh R, Nakamura T, Kumar BG, Singh RP, Nakamura T. Degradation of carbon fiber-reinforced epoxy composites by ultraviolet radiation and condensation. J Compos Mater 2002;36(24):2713–33.
[18] Mukhrejee A, Arwikar S. Performance of externally bonded GFRP sheets on concrete in tropical environments. Part I: Structural scale tests. Compos Struct 2007;81(1):21–32.
[19] Hashim M. Durability and performance of carbon fiber reinforced polymer-concrete bonding system under tropical climate. Johor Bahru: Universiti Teknologi Malaysia; 2010. p. 325.
[20] De Lorenzis L, Miller B, Nanni A. Bond of FRP laminates to concrete. ACI Mater J 2001;98(3):256–64.
[21] Etman E, Beeby A. Experimental programme and analytical study of bond stress distributions on a composite plate bonded to a reinforced concrete beam. Cement Concr Compos 2000;22:281–91.
[22] Mukhopadhyaya P, Swamy R. Interface shear stress: a new design criterion for plate debonding. J Compos Constr 2001;5(1):35–43.
[23] Mukhopadhaya P, Swamy R, Lynsdale C. Influence of aggressive exposure conditions on the behaviour of adhesive bonded concrete – GFRP joints. Constr Build Mater 1998;12:427–46.
[24] Chen J, Teng J. Anchorage strength models for FRP and steel plates bonded to concrete. J Struct Eng 2001;127(7):784–91.
[25] Buyukozturk O, Gunes O, Karaca E. Progress on understanding debonding problems in reinforced concrete and steel members strengthened using FRP composites. Constr Build Mater 2004;18(1):9–19.
[26] Yao J, Teng J, Chen J. Experimental study on FRP-to-concrete bonded joints. Compos B Eng 2005;36(2):99–113.
[27] Xiao J, Li J, Zha Q. Experimental study on bond behavior between FRP and concrete. Constr Build Mater 2004;18(10):745–52.
[28] Cao S, Chen J, Pan J, Sun N. ESPI measurement of bond-slip relationships of FRP-concrete interface. J Compos Constr 2007;11(2):149–60.
[29] "ASTM D3039/D3039M-95a". In: Annual book of ASTM standard test method for tensile properties of polymer matrix composite materials. vol. 15.03, 1995. p. 43–45.
[30] Arcan M, Hashin Z, Voloshin A. A method to produce uniform plane-stress states with applications to fibre-reinforced materials. Exp Tech 1978:141–6.
[31] Malaysian Meteorological Department. Official website, Available: http://www.met.gov.my.
[32] Singh M, Adams R. Low temperature transitions in fibre reinforced polymers. J Compos A 2001;32:797–814.
[33] Bizindavyi L, Neale K. Transfer lengths and bond strengths for composites bonded to concrete. J Compos Constr 1999;3(4):153–60.
[34] Chajes M, Finch W, Januszka T, Thomson T. Bond and force transfer of composite material plates bonded to concrete. ACI Struct J 1996:208–17.
[35] Austin S, Robins P, Pan Y. Shear bond testing of concrete repairs. Cem Concr Res 1999;29:1067–76.